

Solubility of NaCl in water by molecular simulation revisited

J. L. Aragoles, E. Sanz, and C. Vega

Citation: *J. Chem. Phys.* **136**, 244508 (2012); doi: 10.1063/1.4728163

View online: <http://dx.doi.org/10.1063/1.4728163>

View Table of Contents: <http://jcp.aip.org/resource/1/JCPSA6/v136/i24>

Published by the [American Institute of Physics](#).

Additional information on *J. Chem. Phys.*

Journal Homepage: <http://jcp.aip.org/>

Journal Information: http://jcp.aip.org/about/about_the_journal

Top downloads: http://jcp.aip.org/features/most_downloaded

Information for Authors: <http://jcp.aip.org/authors>

ADVERTISEMENT



ACCELERATE AMBER AND NAMD BY 5X.
TRY IT ON A FREE, REMOTELY-HOSTED CLUSTER.

LEARN MORE

Solubility of NaCl in water by molecular simulation revisited

J. L. Aragones, E. Sanz, and C. Vega^{a)}

Departamento de Química Física, Facultad de Ciencias Químicas, Universidad Complutense de Madrid, 28040 Madrid, Spain

(Received 29 March 2012; accepted 24 May 2012; published online 27 June 2012)

In this paper, the solubility of NaCl in water is evaluated by using computer simulations for three different force fields. The condition of chemical equilibrium (i.e., equal chemical potential of the salt in the solid and in the solution) is obtained at room temperature and pressure to determine the solubility of the salt. We used the same methodology that was described in our previous work [E. Sanz and C. Vega, *J. Chem. Phys.* **126**, 014507 (2007)] although several modifications were introduced to improve the accuracy of the calculations. It is found that the predictions of the solubility are quite sensitive to the details of the force field used. Certain force fields underestimate the experimental solubility of NaCl in water by a factor of four, whereas the predictions of other force fields are within 20% of the experimental value. Direct coexistence molecular dynamic simulations were also performed to determine the solubility of the salt. Reasonable agreement was found between the solubility obtained from free energy calculations and that obtained from direct coexistence simulations. This work shows that the evaluation of the solubility of salts in water can now be performed in computer simulations. The solubility depends on the ion-ion, ion-water, and water-water interactions. For this reason, the prediction of the solubility can be quite useful in future work to develop force fields for ions in water. © 2012 American Institute of Physics. [<http://dx.doi.org/10.1063/1.4728163>]

INTRODUCTION

When a soluble salt is added to water, there is a point where further addition of salt does not increase the concentration of salt dissolved in water. Any extra amount of salt added simply precipitates and goes to the bottom of the vessel. The equilibrium concentration of salt dissolved in water in equilibrium with the solid phase of the salt is denoted as the solubility limit of the salt, or simply the solubility. The value of the solubility depends on the salt, the solvent, and the thermodynamic conditions (i.e., the temperature and pressure). The presence of salts significantly modifies the properties of pure water, and also affects the properties of biological molecules in water.¹⁻³ Many experimental studies have been performed to analyze these issues.^{4,5} Experimental studies of both thermodynamic and kinetic aspects of the equilibrium between salts and their saturated solutions are also crucial in geological studies.⁶⁻¹⁰ Sodium chloride (NaCl) is one of the most abundant salts available on earth, and for this reason many experimental studies have been devoted to determining the properties of NaCl solutions, and the effect of NaCl on biological molecules.^{11,12} It is clear that computer simulations can complement these studies by supplying a molecular perspective of the behavior of the system. For this reason, many of the simulation studies have been devoted to NaCl solutions¹³⁻²⁴ and primitive models of ionic systems.^{25,26} The chemical potential of ions in solution has been calculated in many simulation studies.²⁷⁻³¹ However, it is somewhat surprising to realize that the number of studies devoted to determine from molecular simulations the solubility of salts into water is quite small. Ferrario *et al.* determined for the first time the solubil-

ity of KF into water using computer simulations.³² Later on, Sanz and Vega determined the solubility of NaCl into water.³³ The interest in the problem seems to be growing in the last few years. In fact, in 2010 Maginn and co-workers determined the solubility of NaCl in water,³⁴ and quite recently another paper by Lisal and co-workers on the same problem appeared.³⁵ This recent activity provides some indication that the interest in this problem may increase significantly in the near future. Why is the number of computer simulation studies on solubility so small? In our opinion, the main reason for this is that determining the solubility of a salt in water by computer simulation is not an easy problem. The common route to evaluate the solubility by computer simulation is to determine the chemical potential of the salt in the solid phase and the chemical potential of the salt into water as a function of the composition of the solution. The composition of the solution at which the chemical potential of the salt is identical to that of the pure solid (at a certain T and p) determines the solubility of the salt. Why is that so involved? First, because determining the chemical potential of the salt in the solid phase requires in general using special techniques such as the Einstein crystal³⁶ or Einstein molecule method^{37,38} that are generally not implemented in standard molecular dynamics (MD) programs. Second, the evaluation of the chemical potential of the salt in water is far from trivial, and an accurate evaluation is needed to have a reasonable estimate of the solubility.

Direct coexistence simulations could be an alternative route. The methodology proposed by Ladd and Woodcock has been implemented successfully to the Lennard-Jones (LJ) system.^{39,40} It can be also used for molecular fluids as water as shown by Haymet and Karim⁴¹ and Fernandez *et al.*⁴² For the ice Ih-water equilibrium, we have obtained that the

^{a)}cvega@quim.ucm.es.

melting point temperature obtained from free energy calculations (i.e., the thermodynamic route) is identical within the error bar to that obtained from direct coexistence simulations.⁴³ That constitutes a crosscheck of the robustness of the calculations. To the best of our knowledge, the only study of the solubility problem by direct coexistence simulations was undertaken by Joung and Cheatham (JC).⁴⁴

The first goal of this paper is methodological. We shall evaluate the solubility of NaCl in water by a thermodynamic route, following the methodology described in our previous work³³ after incorporating some improvements. We shall also determine the solubility from direct coexistence simulations, to illustrate that there is reasonable agreement between the two routes. There is a second motivation for this study. When modeling the solubility of NaCl in water, it is necessary to define the potential used for ion–ion, ion–water, and water–water interactions. The set of these three potentials will be denoted as the “force field.” Since force fields provide only an approximate description of molecular interactions, there is no guarantee that the solubility evaluated by a force field will match the experimental value. In this work, we shall explore how much the solubility of NaCl in water differs for different force fields. It will be shown that the solubility obtained for the considered force fields may be quite different. These are bad news since it means that the disagreement with the experimental values can be quite large. However, the sensitivity of the solubility to the force field can be used to discriminate between “good” and “bad” force fields, at least with respect to the solubility problem. It will be shown here that the model proposed by Joung and Cheatham⁴⁵ provides a reasonable estimate of the solubility of NaCl into water. This model represents an improvement with respect to previous models. It is our impression that there is still room for improvement in the area of force field developments for salts in water, and that the solubility could be used as a target property in the development of force fields for this kind of systems.

In summary, in this work we shall try to illustrate that the evaluation of the solubility of NaCl into water by computer simulation is feasible using current computational resources, and that results obtained from thermodynamic integration are reasonably consistent with those obtained from direct coexistence simulations. Also it will be shown that one of the studied models provides a quite reasonable estimate of the solubility of NaCl in water. We do hope that this work attracts more researchers into the interesting problem of the determination of the solubility of salts into water by computer simulation.

MOLECULAR MODELS

In this work, the solubility of NaCl in water has been determined for three different force fields. In all cases, the SPC/E model⁴⁶ was used to describe the water–water interactions. All previous studies dealing with the solubility of NaCl in water used this water model, so that our choice allows a comparison with the results of other authors. In the SPC/E model, positive charges are located on the position of the hydrogen atoms and a negative charge is located on the position of the oxygen atom. Besides the charges, a LJ potential is located on the oxygen atom (Table I). For this model, the water

TABLE I. Parameters for the Smith–Dang, Joung–Cheatham, and Tosi–Fumi force fields. The crossed interactions are obtained by the Lorentz–Bertheloth combining rules for SD and JC force fields.

LJ interaction	ϵ/k_B (K)	σ (Å)	Charge	q (e)
Water SPC/E				
O–O	78.20	3.166	O	−0.8476
			H	0.4238
Smith–Dang				
Na ⁺ –Na ⁺	65.42	2.35	Na ⁺	+1.0
Cl [−] –Cl [−]	50.32	4.40	Cl [−]	−1.0
Na ⁺ –Cl [−]	57.375	3.375		
Na ⁺ –O	71.525	2.758		
Cl [−] –O	62.730	3.783		
Joung–Cheatham				
Na ⁺ –Na ⁺	177.457	2.159	Na ⁺	+1.0
Cl [−] –Cl [−]	6.434	4.830	Cl [−]	−1.0
Na ⁺ –Cl [−]	33.789	3.495		
Na ⁺ –O	117.841	2.663		
Cl [−] –O	22.430	3.998		
Tosi–Fumi				
Na ⁺ –O	71.52	2.758	Na ⁺	+1.0
Cl [−] –O	62.73	3.783	Cl [−]	−1.0

molecule geometry is $d(\text{OH}) = 1 \text{ \AA}$ and $\theta(\text{HOH}) = 109.47$. Let us now present the three force fields considered in this work. In all cases, a positive charge of magnitude e and a negative charge $-e$ are located on the position of the Na⁺ cation and Cl[−] anion, respectively. However, the force fields differ in the way that the non-Coulombic part of the ion–ion or ion–water interactions are described.

Force field I (TF)

In the first force field considered in this work, the ion–ion interactions are described by the potential proposed by Tosi and Fumi (TF) for alkaline halides.^{47–50} The potential parameters were fitted to reproduce properties of the pure solid, and for this reason the Tosi–Fumi potential is commonly used in studies of pure salts and melts of ionic systems.^{51–53} The ion–ion potential is given by the expression

$$u_{ij} = A_{ij}e^{-r_{ij}/\rho_{ij}} - \frac{C_{ij}}{r_{ij}^6} - \frac{D_{ij}}{r_{ij}^8} + \frac{q_i q_j}{4\pi\epsilon_0 r_{ij}}. \quad (1)$$

The parameters of the ion–ion interactions for NaCl were described in detail in Ref. 33. Since the Tosi–Fumi potential was aimed to describe pure NaCl, these authors did not provide parameters to describe the water–ion interaction. In their pioneering study of solubility, Ferrario *et al.*³² used the Tosi–Fumi potential to describe the ion–ion interactions (in KF) and a LJ potential to describe the ion–water interactions using the parameters proposed by Smith and Dang (SD).⁵⁴ This route was also followed by several authors for NaCl.^{33–35} Thus, the first force field considered in this work, which will be denoted as “TF,” is “hybrid” in the sense that uses the Tosi–Fumi potential for ion–ion interactions and a LJ type

for water–ion interactions. The parameters for the ion–water interactions of the TF potential are presented in Table I.

Force field II (SD)

For the second force field considered in this work, both the ion–ion and the ion–water interactions are described by the Lennard–Jones potential. For NaCl in SPC/E water, the parameters are presented in Table I, and they have taken directly from the original paper of Smith and Dang.^{54,55} This force field will simply be denoted as “SD.” It is interesting to point out that in the SD force field the ion–water interactions are simply a consequence of applying the Lorentz–Berthelot combining rules to the ion–ion and water–water interactions. This force field is quite popular in studies of NaCl in water although somewhat surprisingly the solubility of this model has never been computed before.

Force field III (JC)

This force field is similar in spirit to the SD force field. Again the ion–ion and ion–water interactions are described by a LJ potential. Joung and Cheatham proposed a set of NaCl force field each one tailored for the model considered to describe water.⁴⁵ Here, we shall focus on the parameters of NaCl in SPC/E water to be consistent with the rest of the results of the paper. Interestingly, even though Joung and Cheatham used a LJ potential to describe ion–ion and ion–water interactions and the SPC/E to describe water, they proposed a set of parameters completely different from those proposed by Smith and Dang.⁵⁴ The parameters of this force field are presented in Table I. We shall denote this force field as “JC.”

SOLUBILITY OF SALTS FROM FREE ENERGY CALCULATIONS

The solubility limit of a salt AX at a certain temperature and pressure is just the concentration of the salt at which the chemical potential of the salt in the solution $\mu_{AX}^{\text{solution}}$ becomes identical to that of the pure solid μ_{AX}^{solid}

$$\mu_{AX}^{\text{solid}} = \mu_{AX}^{\text{solution}}. \quad (2)$$

In this work, we shall determine the solubility of NaCl in water at room temperature (298 K) and normal pressure (1 bar). For a certain phase, let us denote as N_A the number of cations of a system, N_X the number of anions, and N_{AX} the number of molecules of salt. Obviously it always holds that (if the salt is A_iX_j with $i = j = 1$)

$$N_A = N_X = N_{AX}. \quad (3)$$

Let us denote as N the total number of particles of a certain phase. For the salt in the solid phases it holds

$$N = N_A + N_X = 2N_{AX} \quad (4)$$

whereas for a solution of AX in water N is given by

$$N = N_A + N_X + N_{H_2O}. \quad (5)$$

Let us first describe the procedure to obtain the chemical potential of salt in the solid phase.

Chemical potential of AX in the solid phase

The chemical potential of AX in the solid phase is simply

$$\mu_{AX}^{\text{solid}} = \left(\frac{G_{\text{solid}}}{N_{AX}} \right) = \left(\frac{A_{\text{solid}} + pV_{\text{solid}}}{N_{AX}} \right). \quad (6)$$

By performing NpT simulations of the AX solid at room temperature and pressure, it is possible to determine easily V_{solid} . The term A_{solid} can be computed by using the Einstein crystal³⁶ or Einstein molecule^{37,38} methodologies. In these methodologies, NVT simulations are performed in which the Hamiltonian of the system is modified from the original solid to one for which the free energy can be computed analytically. Both in the Einstein crystal and Einstein molecule methodologies, the reference system consists of non-interacting particles connected to the equilibrium lattice positions by harmonic springs (hence the name Einstein crystal). In the Einstein crystal, the center of mass of the system is fixed, whereas in the Einstein molecule the center of mass of just one particle in the system remains fixed. The calculations are performed at the equilibrium density of the system at the considered temperature and pressure. The final expression of the Helmholtz free energy of the solid of Einstein crystal/molecule calculations is⁵⁶

$$A = A_0 + \Delta A_1 + \Delta A_2. \quad (7)$$

The term A_0 is the free energy of the reference system. The analytical expression for A_0 is slightly different in the Einstein crystal and Einstein molecule methodologies.⁵⁶ The term ΔA_1 is just the difference in free energy between an Einstein crystal/molecule with no intermolecular interactions and an Einstein crystal/molecule with intermolecular interactions. The expression used to compute ΔA_1 is the same in the Einstein crystal and Einstein molecule methodologies, being the only difference the choice of the reference point that remains fixed (center of mass of the system or center of mass of a reference particle). The term ΔA_2 gives the free energy difference between the considered solid and a system with intermolecular interactions and additional harmonic springs (of strength Λ_E) connecting the atoms to the equilibrium lattice positions. Again, the expression for ΔA_2 is the same in Einstein crystal/molecule calculations, the only difference being the choice of the particle that remains fixed. We refer the reader to the original references for further details, and specially to our review about free energy calculation of solid where the expression and all technical details are provided.⁵⁶ It is convenient to assume that the thermal de Broglie wavelength of all species is $\Lambda_b = 1 \text{ \AA}$, and that the rotational, vibrational, and electronic partition function of all species is one. As discussed in our previous work,⁵⁶ these arbitrary choices affect the value of the free energy but does not affect phase equilibria (provided the same choice is adopted in all phases). Let us point out that free energies obtained from Einstein crystal calculations are identical to that obtained from free Einstein molecule calculations. The free energy of a solid is unique and does not depend on the computational details. We found that this was indeed the case for hard spheres.³⁷ The same was found here for NaCl. We computed in all cases the free energy of the solid AX from

Einstein crystal and Einstein molecule calculations and found that the free energies obtained by both routes was the same to within the statistical uncertainty. That was also a crosscheck of the calculations since it means that we have computed the free energy of the solid by two somewhat different routes.

The chemical potential of AX in the water phase

The procedure to obtain the chemical potential of the AX salt in solution used in this work is basically that first proposed by Sanz and Vega.³³ However, as will be discussed later some technical details about the practical implementation of the method will differ from the original work. We shall first describe the methodology, and discuss later on the details about how it was implemented in this work.

The chemical potential of an AX salt in water is defined as

$$\mu_{\text{AX}}^{\text{solution}} = \left(\frac{\partial G_{\text{solution}}}{\partial N_{\text{AX}}} \right)_{T,p,N_{\text{H}_2\text{O}}}, \quad (8)$$

where G_{solution} is the total Gibbs free energy of the solution and N_{AX} is the number of molecules of salt in the solution. Notice that the number of water molecules should be constant when computing the derivative of the previous expression, in this work $N_{\text{H}_2\text{O}} = 270$. As usual, the Gibbs free energy of the solution is obtained from the sum of the Helmholtz free energy A_{solution} and of the pV_{solution} term

$$G_{\text{solution}} = A_{\text{solution}} + pV_{\text{solution}}. \quad (9)$$

In short, our strategy is to compute A_{solution} and pV_{solution} for several solutions differing in the number of NaCl molecules N_{AX} but with the same number of water molecules $N_{\text{H}_2\text{O}}$. From the computed value of G_{solution} the chemical potential of the salt in the solution is obtained by the derivative of Eq. (8). The pV_{solution} term is obtained easily from the NpT runs. Then, the cumbersome job is to compute A_{solution} . The total Helmholtz free energy of the solution can be divided into an ideal and a residual term. A residual property is defined as that of the real system at the considered thermodynamic state and that of an ideal system at the same temperature, density, and composition

$$A_{\text{solution}} = A_{\text{solution}}^{\text{id}} + A_{\text{solution}}^{\text{res}}. \quad (10)$$

The ideal term is obtained from the expression⁵⁷

$$\frac{A_{\text{solution}}^{\text{id}}}{k_B T} = N_{\text{H}_2\text{O}} \ln(\rho_{\text{H}_2\text{O}} \Lambda_b^3) + 2N_{\text{NaCl}} \ln(\rho_{\text{NaCl}} \Lambda_b^3) - N_{\text{H}_2\text{O}} - 2N_{\text{NaCl}}, \quad (11)$$

where $\rho_i = \frac{N_i}{V}$ and where we have chosen the de Broglie thermal wavelength of all species to be $\Lambda_b = 1 \text{ \AA}$ and set the internal partition function of all species to one to be consistent with our previous choice for the solid phase. Notice that we are treating the NaCl water solution as a ternary mixture (although in practice we always take into account that $N_A = N_X$). To compute $A_{\text{solution}}^{\text{res}}$, the NaCl water solution is transformed into a pure Lennard–Jones fluid for which the residual free energy is known from the empirical expressions of Kolafa and Nezbeda,⁵⁸ which is basically a reliable fit to

simulation results of the LJ fluid. The transformation of the salt solution in a pure LJ fluid is done via a coupling parameter (λ) in the Hamiltonian of the system. The Hamiltonian of the system is written as a function of λ as

$$U(\lambda) = \lambda U_{\text{LJ},\text{ref}} + (1 - \lambda)U, \quad (12)$$

so that when $\lambda = 1$, the particles of the system interact through a LJ potential and when $\lambda = 0$ one recovers the original salt solution. Then, the residual free energy of the solution can be obtained from Hamiltonian integration as

$$\begin{aligned} A_{\text{solution}}^{\text{res}} &= A_{\text{LJ},\text{ref}}^{\text{res}} + \int_0^1 \langle U - U_{\text{LJ},\text{ref}} \rangle_{N,V,T,\lambda} d\lambda \\ &= A_{\text{LJ},\text{ref}}^{\text{res}} + A^{\text{integral}}. \end{aligned} \quad (13)$$

For each composition, the integrand of the equation above is computed for several values of λ using NVT runs. The value of the volume corresponds to that of the system in the original salt solution at the considered temperature, pressure, and composition. The parameters of the LJ reference system were $\epsilon_{\text{ref}}/k_B = 78.2 \text{ K}$ and $\sigma_{\text{ref}} = 3.14 \text{ \AA}$. We check that no transition was detected along the integration path. Basically, all this methodology is the same as that used by Sanz and Vega.³³ Let us now describe the improvements over our previous methodology that have been used in this work:

- Improvement 1. Very long runs were used to determine the density of NaCl solutions. Either runs of 1×10^6 MC cycles or MD runs of up to 10 ns were used to determine with high accuracy the density of each of the considered solutions.
- Improvement 2. The densities obtained from the NpT runs of the solutions were fitted to a polynomial expression as a function of N_{NaCl} . That reduces the noise of each density and probably reduces also the error in the estimate of the density for each composition.
- Improvement 3. The error in the estimate of A_{solution} was reduced significantly. That was consequence of several changes. First, since A_{solution} is computed in NVT runs, the more accurate value of V obtained from the two previous improvements certainly helped to increase the accuracy of the estimate of A_{solution} . Second, longer NVT runs were used to evaluate the integrand of Eq. (13). While in our previous work we used runs of 20 000 + 30 000 cycles, here we used runs of 80 000 + 100 000 cycles. A cycle was defined as a trial move per particle of the system (translation or rotation in the case of water) plus a trial volume change (in the case of NpT runs). Another important feature is that we increased the number of values of λ considered to evaluate the integrand. Whereas in our earlier paper we used Gaussian integration with 11 values of λ , here we have used Simpson integration and the number of values of λ has been increased to 21. The use of Simpson's integration allows more values of λ in regions where the integrand of Eq. (13) changes abruptly (region of λ values between 0.95 and 1). Besides since the final configuration of each value of λ was used as initial configuration of the following value of λ , this also

helps significantly the equilibration of the system. In summary, we have increased the accuracy computing A_{solution} .

- Improvement 4. This improvement concerns the evaluation of the derivative of Eq. (8), which yields the chemical potential of the salt. In our previous work, we fitted G_{solution} to a quadratic function of N_{AX} . As a consequence, the chemical potential became a linear function of N_{AX} . This is fine when considering a narrow range of concentrations (and that was indeed the aim of our original approach). But it is true that the chemical potential of NaCl in water presents a strong curvature at small concentrations, and this feature (consequence of logarithmic terms in the ideal contribution to the free energy) is not reproduced by the way we performed the analysis. For this reason, Lisal *et al.*³⁵ and Maginn *et al.*³⁴ have criticized the approach used in our previous study. We admit the criticism and we have modified the way the chemical potential is obtained. Let us re-write G_{solution} as

$$\begin{aligned} G_{\text{solution}} &= A_{\text{solution}}^{\text{id}} + [A_{\text{solution}}^{\text{res}} + pV_{\text{solution}}] \\ &= G_1 + [G_2]. \end{aligned} \quad (14)$$

We have found that G_2 can be fitted quite well by a quadratic function of N_{AX} (it should be noticed that the pV_{solution} term is quite small as compared to the term $A_{\text{solution}}^{\text{res}}$) so that

$$G_2 = A_{\text{solution}}^{\text{res}} + pV_{\text{solution}} = a + bN_{\text{NaCl}} + cN_{\text{NaCl}}^2. \quad (15)$$

According to this, the contribution of these two terms (i.e., G_2) to the chemical potential of NaCl in the solution, which we shall denote as $\mu_{\text{NaCl},2}^{\text{solution}}$ is simply

$$\mu_{\text{NaCl},2}^{\text{solution}} = b + 2cN_{\text{NaCl}}. \quad (16)$$

The second contribution to the chemical potential $\mu_{\text{NaCl},1}^{\text{solution}}$ is given by

$$\mu_{\text{NaCl},1}^{\text{solution}} = \left(\frac{\partial A_{\text{solution}}^{\text{id}}}{\partial N_{\text{AX}}} \right)_{T,p,N_{\text{H}_2\text{O}}}. \quad (17)$$

It is possible to show that $\mu_{\text{NaCl},1}^{\text{solution}}$ is given by (see Appendix A)

$$\begin{aligned} \mu_{\text{NaCl},1}^{\text{solution}} &= \left(\frac{\partial A_{\text{solution}}^{\text{id}}}{\partial N_{\text{NaCl}}} \right)_{T,p,N_{\text{H}_2\text{O}}} \\ &= 2k_B T \ln(\rho_{\text{NaCl}}) - k_B T \bar{V}(\rho_{\text{H}_2\text{O}} + 2\rho_{\text{NaCl}}), \end{aligned} \quad (18)$$

where \bar{V} is the partial molar volume of NaCl ($\bar{V} = \left(\frac{\partial V}{\partial N_{\text{NaCl}}} \right)_{T,p,N_{\text{H}_2\text{O}}}$). Notice that the derivative of the ideal Helmholtz free energy is performed while keeping T , p , and $N_{\text{H}_2\text{O}}$ constant (and not while keeping T , V , and $N_{\text{H}_2\text{O}}$ constant). That explains the appearance of a partial volume contribution (see Appendix A). To calculate Eq. (18), we get ρ_{NaCl} , \bar{V} , and $\rho_{\text{H}_2\text{O}}$ from the ρ_{NaCl} as given from the fit described

in “improvement 2.” We have checked that this is fully equivalent to evaluate numerically the derivative given by Eq. (17). The total chemical potential of NaCl in the solution is obtained easily by adding these two contributions

$$\mu_{\text{NaCl}}^{\text{solution}} = \mu_{\text{NaCl},1}^{\text{solution}} + \mu_{\text{NaCl},2}^{\text{solution}}. \quad (19)$$

For all simulations aimed to compute the chemical potential of NaCl in the solution, Ewald sums were used to deal with Coulombic interactions. The LJ and the real part of the Coulombic interactions were truncated at $r_c = 9 \text{ \AA}$. A home made program was used. We checked that the results are totally consistent with those obtained from the MD package GROMACS (Ref. 59) (see Appendix C). Standard corrections for the truncation of the potential were used for the LJ contribution. In the Ewald sums, the term controlling the convergence of the reciprocal space sum was chosen so that ($\alpha \cdot r_c = 2.98, 0.29 \text{ \AA}^{-1}$ for a cutoff of $r_c = 9 \text{ \AA}$). All NpT runs used isotropic scaling since we are dealing either with fluid phases or with cubic crystals (with the NaCl cubic structure).

Direct coexistence simulations

Experimentally, when a large amount of solid NaCl is introduced into water, one finds that after a certain amount of time, part of the NaCl dissolves into water, and the two phases (the solid NaCl and the NaCl solution) reaches the equilibrium. Then the concentration of NaCl in the solution reach the solubility limit. That opens a possible route to determine the solubility of NaCl in water in computer simulations. A block of NaCl is introduced in one side of the simulation box, and water is introduced in the other side, and molecular dynamics simulations are performed until the system reaches the equilibrium. We performed MD simulations by putting pure NaCl in contact with pure water. Unfortunately, this approach was not very useful as no single ion from the solid went to the fluid phase even after 500 ns. What is the reason for this “apparent” disagreement between experiment and simulation? The reason is that the solution of solid NaCl into water is a “rare event,” since it has a high activation energy and it is necessary to wait times much longer than those used typically in computer simulations to see it. For this reason, this does not seem to be a very useful route to determine solubilities (it remains to be studied in future studies if the introduction of defects, kinks, steps or even roughness on the surface of solid NaCl could help to reduce the time required to see the migration of ions from the solid to the solution). The second possibility is to introduce solid NaCl in one side of the simulation box and a supersaturated water solution in the other side. Since the solution in supersaturated part of the ions in the solution will precipitate, or in other words will incorporate to the solid phase until the system reaches the equilibrium concentration. Can this second route work? This second route was recently employed by Joung and Cheatham.⁴⁴ It will be shown in this work that this second route can indeed be used to determine the solubility, although long runs, of the order of several microseconds, are needed (at least

for the force fields of NaCl considered in this work). The reason why still long runs are needed is that the incorporation of ions from the supersaturated solution to the solid phase is still an activated process with a free energy of activation. In fact, the ions must get rid of part of the first solvation layer of water molecules before incorporating into the crystal. However, it is likely that the activation energy of this process is lower than the activation energy of the opposite one.

Let us now provide some details about direct coexistence (NaCl solid–supersaturated solution) runs. Molecular dynamic simulations were performed using GROMACS (Ref. 59) (version 4.5). Direct coexistence simulations were performed for the SD and JC force fields. A velocity scaling thermostat⁶⁰ was used to keep T fixed and a Parrinello–Rahman barostat⁶¹ was used to keep pressure constant. The shape of the simulation box was orthorhombic and the three sides of the simulation box were allowed to vary independently, to avoid the presence of any stress in the solid phase (stress could change the free energy of the solid and affect the solubility). The relaxation time for the thermostat and barostat was of 2 ps. The time step was 2 fs. The LJ interaction was truncated at 8.5 Å and standard long range correction was employed. Ewald sums were used to deal with the Coulombic interactions. The real part of the Coulombic interaction was truncated at 8.5 Å, and the reciprocal contribution was evaluated by using particle mesh Ewald (PME).⁶² The results were obtained by running GROMACS in parallel using 4 CPUs. With this number of processors we typically obtained 30 ns/day so that about 3 months were required to determine the solubility of a given force field. Constraints were used to fix the geometry of the molecule of water by using the algorithm LINCS (Ref. 63) which is quite efficient in runs performed in parallel. The setup of the initial configuration for the MD runs was as follows. The solid NaCl contained in all cases 500 molecules (i.e., 1000 ions). In the case of the SD force field, the supersaturated solution contained 1523 molecules of water and 156 molecules of NaCl (i.e., 312 ions) so that the initial concentration of NaCl in water phase was of about 5.6 m. In the case of JC force field, the supersaturated solution contained 1215 molecules of water and 156 molecules of NaCl (i.e., 312 ions) so that the initial concentration of NaCl in the water phase was of about 7.2 m. Therefore, the number of particles in our simulations was of about 3000. The x direction was perpendicular to the solid NaCl–water interface. The concentration of NaCl in the supersaturated solution was obtained as a function of time as follows. Typically after 200 ns, the average density profile of the individual ions Na^+ and Cl^- in water phase was obtained. In general, the density of Na^+ and Cl^- was found to be a function of x , except for the central region of the water phase (sufficiently far away from the NaCl–water interface) where we found that the concentrations of Na^+ and Cl^- were practically identical as it should be for a bulk NaCl solution. That also guarantees electroneutrality in the central slab of the water solution. The width of this central electroneutral region was typically larger than 20 Å. The molality of NaCl in the solution was obtained by computing the average number density of NaCl and water in this central slab.

TABLE II. Free energy calculations for NaCl solid for Tosi–Fumi (TF), Smith–Dang (SD), and Joung–Cheatham (JC) potential models at 298 K and 1 bar. The free energy reported in the last column corresponds to the sum of all the terms ($A_0 + \Delta A_1 + \Delta A_2$). The spring constant (Λ_E) and the number density $\rho = N/V$ given in particles per Å³ are reported. The number of ions used in the calculations was 1000 and the cutoff was 14 Å. The thermal de Broglie wavelength (Λ_b) was set to 1 Å, and all components of the internal partition function set to one $q_r = q_v = q_e = 1$. These definitions correspond to our reference state 1 (ref 1). EM and EC stands for Einstein molecule and Einstein crystal calculations, respectively.

Model	ρ (N_{ions}/V)	$\Lambda_E/k_B T$ (Å ⁻²)	A_0 ($Nk_B T$)	ΔA_1 ($Nk_B T$)	ΔA_2 ($Nk_B T$)	A^{sol} ($Nk_B T$)
TF(EM)	0.04360	2500	10.006	-156.85	-6.27	-153.11
SD(EC)	0.03981	4000	10.70	-159.90	-6.37	-155.57
JC(EC)	0.04143	4000	10.70	-159.94	-6.34	-155.58

RESULTS

As we have discussed previously, the evaluation of the solubility of NaCl in water involves the calculation of the chemical potential of the salt in the solid phase and in the solution. We shall start by presenting the results for the chemical potential of the pure NaCl solid. The free energy of the NaCl solid was calculated at 298 K and 1 bar by the Einstein crystal/molecule method. The number of ions used in the calculations was $N = 1000$. The potential was truncated at $r_c = 14$ Å, and long range corrections were taken into account by assuming that the radial distribution function was one beyond the cutoff distance. For the TF force field, we implemented the Einstein molecule method, whereas for the SD and JC force fields we used the Einstein crystal method. The different contributions to the Helmholtz free energy (A_0 , ΔA_1 , and ΔA_2) are presented in Table II. The total value of the free energy, which is the sum of these three terms, is presented in the last column of Table II. In our previous work,³³ we calculated the free energy for the TF force field using the Einstein crystal technique. The result of this work, obtained by using the Einstein molecule, is practically identical to that obtained in our previous work. The uncertainty of the free energy calculations presented in this work is of about 0.05 $Nk_B T$ (a quite typical value of the Einstein crystal methodology). To obtain the chemical potential of NaCl in the solid phase, one simply must add the pV term to the Helmholtz free energy obtained by the Einstein crystal/molecule method. At 298 K, the contribution of the pV term is quite small (is of the order of 6×10^{-4} in $Nk_B T$ units), so that G is practically identical to A . The value of the chemical potential of NaCl in the solid phase (given per mol of NaCl) is presented in Table III.

The numerical values of the chemical potential reported in Table III depend on the value of the thermal de Broglie wavelength (Λ_b) and on the value of the partition function of the internal degrees of freedom. In this work, we have set to one the intramolecular partition function and to 1 Å the thermal de Broglie wavelength, labeled as reference state 1 ($\mu_{\text{NaCl}}^{\text{sol}, \text{ref}1}$). Although this arbitrary choice does not affect phase equilibria (provided the same value is used for all phases), it does not allow a comparison with the experimental values of the chemical potential. It is necessary to correct

TABLE III. Chemical potential for the NaCl solid at 298 K and 1 bar for TF, SD, and JD models. The first column corresponds to the chemical potential of the solid using our choice of reference system ($\mu_{\text{NaCl}}^{\text{sol,ref1}}$), and the second column are the shifted values of the chemical potential in order to compare with the experimental value ($\mu_{\text{NaCl}}^{\text{sol,ref2}}$). The experimental value was taken from Ref. 64.

Model	$\mu_{\text{NaCl}}^{\text{sol,ref1}}$ (kJ mol ⁻¹)	$\mu_{\text{NaCl}}^{\text{sol,ref2}}$ (kJ mol ⁻¹)
TS	-758.68	-371.88
SD	-770.87	-384.07
JC	-770.92	-384.12
Exp.	-770.82	-384.02

our simulation results for the different choice of the reference system used in experiments and in this work. This is simply done by adding 386.8 kJ/mol to the simulations results, and correspond to the reference state 2 ($\mu_{\text{NaCl}}^{\text{sol,ref2}}$). The justification of the value of the shift is described in detail in Appendix B. As can be seen, the SD and JC force fields reproduce almost exactly the experimental value of the chemical potential. However, the TF force field provides a value that is about 12 kJ/mol higher (about 2%). It is interesting to note that the chemical potential of NaCl in the solid phase was not used as a target property for determining the potential parameters of the SD and JC force field (and the same is true for the TF force field). The fact that these two force fields, SD and JC, reproduces the experimental value of the chemical potential of the solid should be regarded as a successful prediction of these two models.

We shall now discuss the results for the NaCl solutions. In Fig. 1, experimental density of the NaCl in water is compared to the simulation results for the three force fields considered in this work. The predictions of the TF and SD force fields are quite similar and agree quite well with the experimental values for concentrations up to 4 m. For higher concentrations, these two models seem to underestimate the experimental values. The TF and SD force fields have different ion-ion interactions but the same water-ion interactions. At low concentrations of salt, the ion-ion interactions play a minor role. Ion-ion interactions become increasingly important

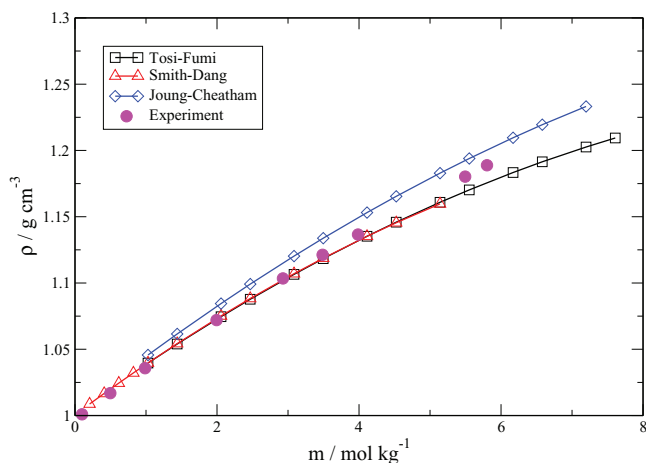


FIG. 1. Density versus NaCl molality for the considered force fields compared to the experimental values (as indicated in the legend).

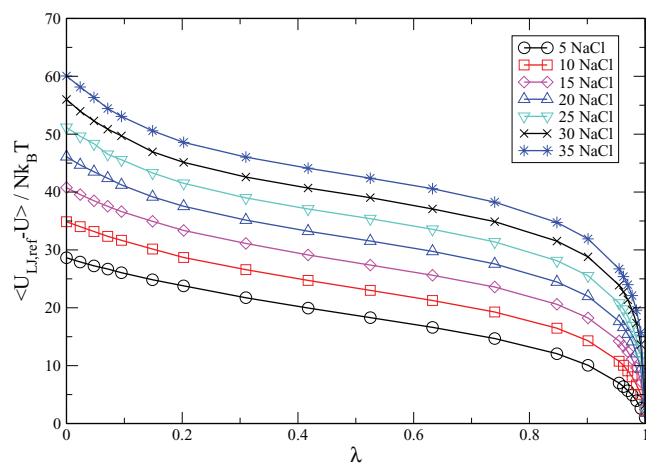


FIG. 2. Integrand of the transformation of Joung-Cheatham NaCl solution into a Lennard-Jones fluid for several NaCl solutions.

as the concentration of the salt increases. The density prediction of the JC force field tends to overestimate the experimental values by a small amount. The densities obtained in this work for the TF force field are quite similar to those reported in our previous work (compare the results of Fig. 1 of this work with those of Fig. 2(a) of our previous work).³³ And in both cases it can be seen that the agreement with experiment is excellent. Paluch *et al.* claimed that our 2007 densities for the TF model did not agree with the experimental values.³⁴ This statement is incorrect as can be seen by simply looking at Fig. 2(a) of our previous work (where the good agreement with experiment is clearly visible), or more simply converting the tabulated results for the number densities reported in Tables IV and V from our previous work to density in g cm⁻³. This can be done simply by using the formula

$$\rho(\text{g/cm}^3) = \rho(N/\text{\AA}^3)(x_{\text{H}_2\text{O}}M_{\text{H}_2\text{O}} + x_{\text{Cl}^-}M_{\text{Cl}^-} + x_{\text{Na}^+}M_{\text{Na}^+}) \times \frac{10^{24}}{N_{\text{Avo}}}, \quad (20)$$

where x_i is the molar fractions of i (treating the system as a ternary mixture) and M_i is the molecular/atomic weight. For example, since we are using 270 molecules of water, for a system with 25 NaCl molecules, the molar fraction of water is $270/(270 + 25 + 25)$ and the molar fraction of Na^+ is $25/(270 + 25 + 25)$. For this reason, the values presented in Fig. 8 of Ref. 34, labeled as Sanz and Vega, are incorrect.

The density varies smoothly as a function of the concentration of salt. For this reason, it seems reasonable to fit the number densities to a quadratic polynomial of the number of NaCl molecules

$$\rho(N/\text{\AA}^3) = d_0 + d_1 N_{\text{NaCl}} + d_2 N_{\text{NaCl}}^2. \quad (21)$$

The coefficients of the fit are presented in Table VI. The NaCl concentration in molality units (mol of NaCl per kilogram of water) can be obtained as

$$m_{\text{NaCl}} = \frac{1000N_{\text{NaCl}}}{N_{\text{H}_2\text{O}}M_{\text{H}_2\text{O}}}. \quad (22)$$

Let us now turn to the calculation of the chemical potential of the solution. Using the fits just described, the density of

TABLE IV. Solution density and terms contributing to the solution Gibbs free energy for the SD model. All the solutions have 270 water molecules. Energies are given in kJ per mol of simulation boxes. The number density $\rho = N/V$ is given in particles per \AA^3 . The chemical potential of NaCl is given in kJ per mol of NaCl.

N_{NaCl}	ρ	G_{solution}	A^{integral}	$A_{\text{LJ},\text{ref}}^{\text{res}}$	pV_{solution}	$A_{\text{solution}}^{\text{id}}$	m (mol kg^{-1})	$\mu_{\text{NaCl},\text{ref}2}^{\text{solution}}$ (kJ mol^{-1})
1	0.0 335 566	-11 082.05	-9573.96	1485.61	0.488	-2994.18	0.21	-391.5
2	0.0 336 701	-11 853.53	-10 326.39	1511.91	0.490	-3039.55	0.41	-388.0
3	0.0 337 801	-12 629.48	-11 085.67	1538.10	0.492	-3082.40	0.62	-385.9
4	0.0 338 866	-13 404.25	-11 845.24	1564.15	0.494	-3123.65	0.82	-384.5
5	0.0 340 035	-14 174.89	-12 603.93	1592.00	0.496	-3163.45	1.03	-383.3
7	0.0 341 933	-15 700.64	-14 102.38	1642.40	0.500	-3241.16	1.44	-381.5
10	0.0 344 542	-18 017.48	-16 381.43	1716.58	0.507	-3353.14	2.06	-379.5
12	0.0 346 122	-19 545.54	-17 885.33	1764.88	0.511	-3425.60	2.47	-378.5
15	0.0 348 256	-21 833.55	-20 137.47	1835.28	0.519	-3531.88	3.08	-377.2
17	0.0 349 519	-23 383.65	-21 663.36	1880.64	0.524	-3601.45	3.50	-376.4
20	0.0 351 177	-25 634.34	-23 876.56	1946.01	0.531	-3704.32	4.11	-375.4
22	0.0 352 123	-27 173.28	-25 389.36	1987.61	0.537	-3772.07	4.52	-374.9
25	0.0 353 305	-29 468.87	-27 643.45	2046.75	0.545	-3872.71	5.14	-374.1

the NaCl solution was estimated for several numbers of NaCl molecules (remember that the number of water molecules is fixed to 270). The integrand of Eq. (13) was computed by using NVT simulations for different values of λ . In Fig. 2, the integrand is shown for several solutions of the JC force field. In all cases, the integrand is quite smooth in the interval of λ from 0.1 to 0.9. The integrand decreases slightly from 0 to 0.1. On the other hand, the integrand decreases quickly from $\lambda = 0.9$ to $\lambda = 1$. For this reason, we have evaluated the integrand for many values of λ in this region. Notice that the integrand does not diverge either in $\lambda = 0$ nor in $\lambda = 1$. The accuracy obtained in this work for determining the integral of Eq. (13) is higher than in our previous work.³³ The main reasons are that much longer runs were used and that 21 values of λ , distributed reasonably over the integration range, were used instead of the 11 values of lambda employed in our previous work which used Gaussian integration. Once the integral is evaluated, the following step to compute G_{solution} is to add the residual free energy of the LJ reference fluid ($A_{\text{LJ},\text{ref}}^{\text{res}}$),⁵⁸ the

pV_{solution} term and the ideal gas contribution to the Helmholtz free energy (Eq. (14)).

We shall start the discussion by presenting the results for the SD force field. In Tables IV and V, the different contributions to the Gibbs free energy of the solution (ideal, residual, and pV terms) are presented for the SD and TF models. The values reported are free energies expressed in kJ per mol of simulation boxes (neither per mol of water nor per mol of molecules of salt). The value of the pV_{solution} term is quite small compared to the other contributions to the free energy. As described in Eq. (14), the total value of G_{solution} is divided in two contributions. The first one (G_1) is the $A_{\text{solution}}^{\text{id}}$ term, and the second one (G_2) is the sum of the $A_{\text{solution}}^{\text{res}}$ (Eq. (13)) and the pV_{solution} term. G_2 is plotted as a function of the number of molecules of salt (N_{NaCl}) in Fig. 3. The results are quite smooth and can be fitted nicely to a second order polynomial curve of the kind $G_2 = a + bN_{\text{NaCl}} + cN_{\text{NaCl}}^2$. Although not obvious from the figure, we have checked that the sum of squared deviations of the fit is reduced by approximately a

TABLE V. Solution density and terms contributing to the solution Gibbs free energy for the Tosi–Fumi model. All the solutions have 270 water molecules. Energies are given in kJ per mol of simulation boxes. The number density $\rho = N/V$ is given in particles per \AA^3 . The chemical potential of NaCl is given in kJ per mol of NaCl.

N_{NaCl}	ρ	G_{solution}	A^{integral}	$A_{\text{LJ},\text{ref}}^{\text{res}}$	pV	$A_{\text{solution}}^{\text{id}}$	m (mol kg^{-1})	$\mu_{\text{NaCl}}^{\text{solution}}$ (kJ mol^{-1})
5	0.03 399	-14 159.23	-12 586.08	1590.08	0.49	-3163.72	1.03	-382.7
7	0.03 417	-15 696.73	-14 095.41	1639.72	0.49	-3241.53	1.44	-380.6
10	0.03 444	-17 993.39	-16 354.88	1714.42	0.50	-3353.43	2.06	-378.1
12	0.03 460	-19 513.88	-17 851.50	1762.97	0.51	-3425.86	2.47	-376.7
15	0.03 481	-21 818.82	-20 119.88	1832.75	0.52	-3532.21	3.08	-374.9
17	0.03 495	-23 320.83	-21 600.19	1880.33	0.53	-3601.50	3.50	-373.8
20	0.03 512	-25 602.13	-23 844.81	1946.41	0.54	-3704.27	4.11	-372.3
22	0.03 523	-27 137.44	-25 357.01	1990.71	0.54	-3771.68	4.52	-371.3
25	0.03 536	-29 404.79	-27 585.35	2052.06	0.55	-3872.05	5.14	-370.0
27	0.03 544	-30 919.06	-29 073.75	2092.35	0.55	-3938.21	5.55	-369.2
30	0.03 553	-33 197.07	-31 308.67	2147.97	0.56	-4036.93	6.17	-368.0
32	0.03 558	-34 690.91	-32 772.77	2183.55	0.56	-4102.25	6.58	-367.2
35	0.03 563	-36 960.99	-34 994.23	2232.51	0.58	-4199.85	7.20	-366.1
37	0.03 565	-38 433.87	-36 432.55	2262.73	0.59	-4264.64	7.61	-365.4

TABLE VI. Coefficients of the quadratic fits to the number density $\rho(N/\text{\AA}^3)$ (Eq. (21)) as a function of the number of NaCl molecules for the three force fields considered in this work.

Model	$d_0 \times 10$	$d_1 \times 10^3$	$d_2 \times 10^5$
TF	0.3344	0.1149	-0.1507
SD	0.3344	0.1186	-0.1729
JC	0.3355	0.1339	-0.1390

factor of two from the linear to the quadratic fit whereas further increasing the order of the polynomial did not improve significantly the fit. The coefficients of the fit are reported in Table VII. In our previous work,³³ the sum of G_1 and G_2 was fitted to a second order polynomial. That was not a good idea as the G_1 term exhibits a strong curvature. However, it seems quite reasonable to fit the G_2 term to a second order polynomial as it can be seen in Fig. 3. The contribution of G_2 to the chemical potential is obtained from the derivative of G_2 with respect to N_{NaCl} . Therefore, this contribution increases linearly with the number of ions in the solution. The contribution of the ideal term to the chemical potential can be obtained easily by obtaining numerically the derivative of G_1 with respect to N_{NaCl} using the previously described polynomial fit of the number density of the system (Table VI). Alternatively, and certainly more elegantly, one can just compute the partial molar volume of the salt from the fitted values of the densities and using Eq. (18).

Once we have calculated the chemical potential for the solid and for the solution phases we shall estimate the solubility. For the SD force field, the results are presented in Fig. 4. The experimental values of the chemical potential of NaCl, both in the solid phase and in solution, are also shown. The intersection between the experimental values of the chemical potential occurs at a concentration of 6.15 m. This is indeed the experimental value of the the solubility of NaCl in water. The intersection of the chemical potential curves of the SD force field occurs at a concentration of 0.9 m. This differs from the experimental value by about 5.2 units of molality. The solubility of NaCl in water predicted by the SD force field is totally incorrect. Since the SD model predicts correctly the chemical potential of the NaCl solid phase, the problem of

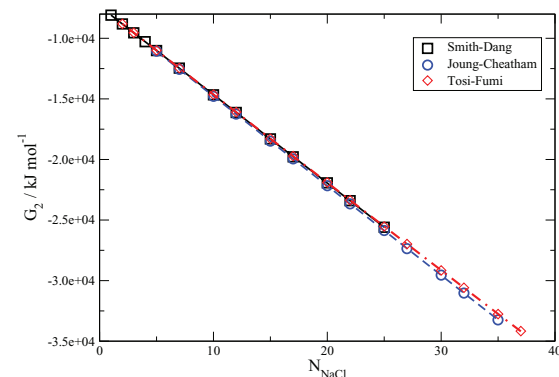


FIG. 3. G_2 contribution to the Gibbs free energy of the solution as a function of the number of NaCl molecules for the three studied force fields. The units of G_2 are kJ per mol of simulation boxes.

TABLE VII. Quadratic fit coefficients of the G_2 ($A_{\text{solution}}^{\text{res}} + pV_{\text{solution}}$) fits for the three force fields. The units of G_2 are kJ per mol of simulation boxes.

Model	$a \times 10^{-4}$	$b \times 10^{-3}$	c
TF	-0.7343	-0.7315	0.1588
SD	-0.7354	-0.7311	0.0692
JC	-0.7365	-0.7426	0.0982

this model is an incorrect prediction of the chemical potential of the salt in the solution, about 12 kJ/mol higher than the experimental value. It is clear from the results of Fig. 4 that the water-ions interactions in the SD force field are somewhat weak, and should be slightly increased to bring the predictions of the model into closer agreement with the experiment. Of course that should be done without modifying the ion-ion interaction, since otherwise the good agreement with the experiment found for the chemical potential of the solid will be lost. The values of the chemical potential of NaCl in the solution reported recently by Lisal *et al.*³⁵ for the SD force field are also presented in Fig. 4. As can be seen our results agree rather well with those of Lisal *et al.*, who use a completely different approach to the calculation of the chemical potential of NaCl in solution. Taking into account the difficulties in the determination of the chemical potential of NaCl in water this is gratifying.

Let us now turn to the results for the JC model. In Table VIII, the different contributions to the Gibbs free energy of the system are provided. Once again, we split G into two contributions, G_1 (which just contains $A_{\text{solution}}^{\text{id}}$) and G_2 with the sum of the other contributions ($A_{\text{solution}}^{\text{res}}$ and pV_{solution} terms). Again G_2 could be fitted nicely to a second order polynomial (Fig. 3) and the coefficients are given in Table VII. Taking the derivative of G_1 and G_2 with respect to N_{NaCl} , and adding these two contributions one obtains the chemical potential of NaCl in water. The chemical potentials of NaCl in the solid phase and in

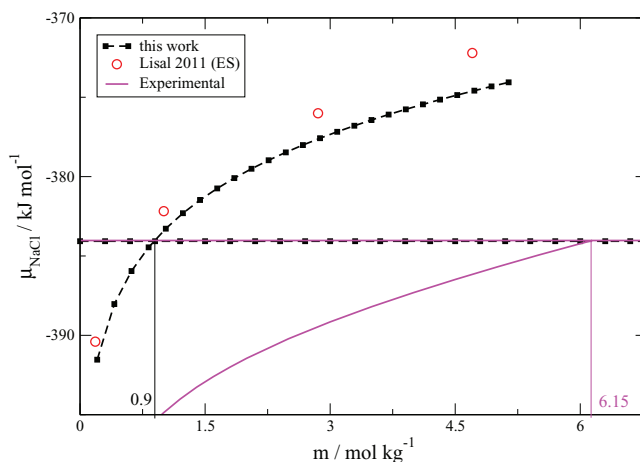


FIG. 4. Chemical potential of NaCl versus molality for the Smith-Dang force field (black dashed line with filled squares). The red open circles represent the results by Lisal *et al.* using Ewald sums.³⁵ The solid magenta curve corresponds with the experimental values. Horizontal lines represent the chemical potential of the solid; experimental (solid line) and Smith-Dang (dashed line with filled squares).

TABLE VIII. Free energy components of Joung–Cheatham NaCl solutions at 298 K and 1 bar. All the solutions have 270 water molecules. Energies are given in kJ per mol of simulation boxes. The number density $\rho = N/V$ is given in particles per \AA^3 . The chemical potential of NaCl is given in kJ per mol of NaCl.

N_{NaCl}	ρ	G_{solution}	A^{integral}	$A_{\text{LJ,ref}}^{\text{res}}$	ρV_{solution}	$A_{\text{solution}}^{\text{id}}$	m (mol kg^{-1})	$\mu_{\text{NaCl}}^{\text{solution,ref}^2}$ (kJ mol^{-1})
5	0.03 419	-14 228.47	-12 687.63	1618.38	0.49	-3159.71	1.03	-394.0
10	0.03 475	-18 136.34	-16 552.57	1762.66	0.50	-3346.94	2.06	-389.9
12	0.03 496	-19 681.54	-18 083.66	1819.95	0.51	-3418.33	2.47	-388.8
15	0.03 525	-22 017.13	-20 399.75	1905.02	0.51	-3522.91	3.08	-387.3
17	0.03 543	-23 540.83	-21 911.05	1960.99	0.52	-3591.28	3.50	-386.4
20	0.03 567	-25 858.95	-24 210.74	2043.49	0.52	-3692.23	4.11	-385.3
22	0.03 583	-27 419.62	-25 758.86	2097.34	0.53	-3758.63	4.52	-384.5
25	0.03 603	-29 725.48	-28 044.94	2176.05	0.53	-3857.13	5.14	-383.5
27	0.03 615	-31 278.67	-29 584.00	2226.97	0.54	-3922.18	5.55	-382.9
30	0.03 632	-33 561.22	-31 843.50	2300.70	0.55	-4018.97	6.17	-382.1
32	0.03 641	-35 111.01	-33 376.39	2347.90	0.55	-4083.07	6.58	-381.5
35	0.03 654	-37 419.88	-35 657.24	2415.48	0.56	-4178.68	7.20	-380.7

the solution are presented in Fig. 5, and compared to the experimental values. As mentioned before, the JC force field predicts quite well the experimental value of the chemical potential of the solid. As to the solution, the predictions for the chemical potential are quite reasonable but slightly higher than the experimental values. The intersect of the two chemical potentials of NaCl occurs at 4.8 m, which is the solubility of NaCl that follows from this force field. This is a quite reasonable result since the experimental value is 6.15 m. The chemical potential of NaCl in solution obtained by Lisal *et al.*³⁵ for the JC force field are also presented in Fig. 5. The agreement with this work is quite good. To estimate the solubility of the JC force field, Lisal *et al.* used the experimental value of the chemical potential of the NaCl solid.³⁵ They estimated the solubility to be 4.8 m, in perfect agreement with our result. The reason for that is that the chemical potential of NaCl in the solid phase for the JC force field is practically identical to the experimental value. Notice also that the approach of Lisal *et al.* could also be used to estimate the

solubility of the SD force field since also for this force field the chemical potential of the model in the solid phase agrees quite well with the experimental value.³⁵ The good news is that there are at least two models (SD and JC) for which the solubility estimated by two different groups agree within the estimated uncertainty of the calculations.

At this point we would like to test the predictions presented so far using a completely different route. The motivation is twofold. First, to guarantee that SD and JC force fields present a dramatically different solubility in water (i.e., 0.9 m and 4.8 m) even though they predict the same chemical potential for the solid phase, close to the experimental value. The second reason is that Joung and Cheatham estimated the solubility for the JC force field using direct coexistence simulations.⁴⁴ They performed simulations of solid NaCl in contact with a supersaturated water solution of NaCl of about 0.4 ns. They estimated that the solubility for the JC force field was 7.2 m. Obviously, this value disagree with the values reported by us and by Lisal *et al.*³⁵ To investigate this in further detail, we performed direct coexistence molecular dynamic runs. At variance with the work of Joung and Cheatham, the length of our runs was of about 2800 ns (this is about 6–8 times longer than the runs of Joung and Cheatham). The time evolution of the bulk density of NaCl in the solution is presented in Fig. 6. The bulk density of NaCl was evaluated in a slab of the solution phase where the effects of the interfaces are negligible. For this reason, it is necessary to carry out simulations with a large number of molecules in the solution phase. The initial solution was supersaturated, and the concentration of the salt decreases with time in the first 1000 ns. That means that one cannot simply run for 200–400 ns to estimate the solubility. Notice that the initial concentration of our runs was just the solubility of the two models predicted by Joung and Cheatham from direct coexistence runs.⁴⁴ After 1.5 μs the concentration of the salt becomes stable, and remains stable for up to one additional microsecond. The results presented in Fig. 6 are quite expensive from a computational point of view. It was required to run GROMACS using 4 CPUs for about 3 months to obtain these curves. Certainly it would be nice to perform even longer runs to be sure that the concentration of

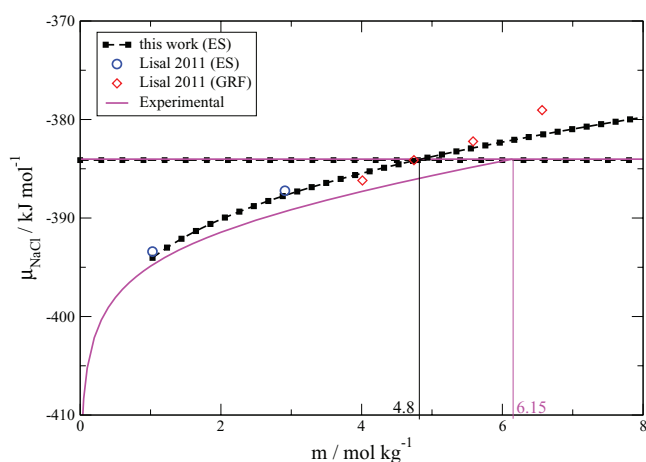


FIG. 5. Chemical potential of NaCl versus molality for the Joung–Cheatham model (black dashed lines with filled squares). The results of Lisal *et al.*³⁵ are represented by blue open circles (Ewald sums) and red open squares (generalized reaction field (GRF)). The magenta solid curve corresponds with the experimental values. Horizontal lines represent the chemical potential of the solid; experimental (solid line) and JC (dashed line with filled squares).

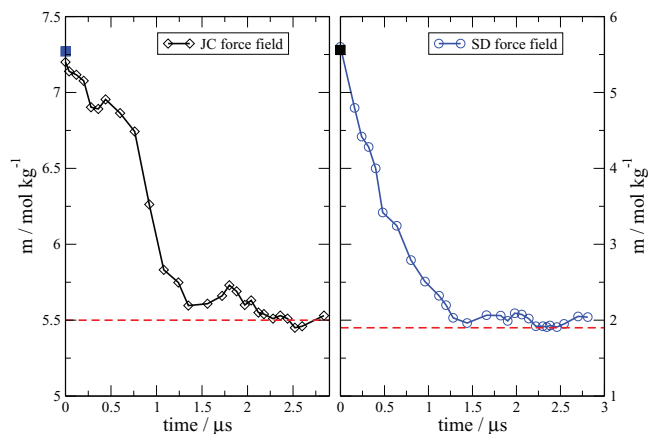


FIG. 6. Molal concentration of NaCl versus simulation time for Smith–Dang (right) and Joung–Cheatham (left) force fields. The filled squares represent the solubility values reported by Joung and Cheatham in Ref. 44. Dashed lines indicate the value at which the molality reaches a plateau.

NaCl in water has reached the equilibrium. However, this is beyond our current computer facilities. For this reason, we shall assume that the plateau of the salt concentration at times above $1.5 \mu\text{s}$ is just the solubility limit obtained from direct coexistence. The plateau in salt concentration cannot be ascribed to dynamical arrest. We have computed the diffusion coefficient of ions and water for the range of concentration considered in this work. The results are shown in Table IX. The water diffusion coefficient decreases as the concentration of salt increases. In fact, the diffusion coefficient of water can decrease up to half its value in the absence of salt. Concerning the ions, the Na^+ presents the smallest diffusion coefficient, its value is roughly one third of water at the same thermodynamic conditions. The diffusion coefficient of Cl^- is slightly higher than that of Na^+ but smaller than that of water. The typical root-mean-square displacement of Na^+ ions in our MD simulations was about 775 \AA . It is clear that the system is not glassy and that the plateau in the concentration versus time profile cannot be due to a dynamic arrest.

The solubility of the SD and JC force fields obtained from free energy calculations and direct coexistence simulations are presented in Table X. The first thing to notice is that direct coexistence simulations indeed confirm that the solubility of the SD force field is about 4 m units smaller than that of the JC model. And second, the difference between the solubility of the SD model from free energy calculations and from direct coexistence simulations is of about 1 m unit. In the case of JC force field, this difference is of about 0.7 m units. Which of the two techniques offer the most reliable val-

TABLE IX. Diffusion coefficients at 298 K and 1 bar for the JD model.

N_{NaCl}	$D_{\text{Na}^+} \times 10^5$ ($\text{cm}^2 \text{ s}^{-1}$)	$D_{\text{Cl}^-} \times 10^5$ ($\text{cm}^2 \text{ s}^{-1}$)	$D_{\text{H}_2\text{O}} \times 10^5$ ($\text{cm}^2 \text{ s}^{-1}$)
10	0.44(9)	0.93(9)	1.61(9)
20	0.40(2)	0.58(9)	1.04(1)
35	0.22(1)	0.26(5)	0.54(4)

TABLE X. Solubility results for the considered force fields.

Model	Solubility (mol kg^{-1})		
	Free energy	Direct coexistence	Recommended
Tosi–Fumi	4.3(3)
Smith–Dang	0.9(4)	1.9(4)	1.4(5)
Joung–Cheatham	4.8(3)	5.5(4)	5.1(3)

ues? We cannot provide a definitive answer to this question. First, the hypothesis that still longer runs are needed in the direct coexistence simulations cannot be definitely ruled out. It could be that the concentration of the salt in the supersaturated solutions occurs quickly initially, when the system is far from equilibrium, and then the process is much slower since the driving force (i.e., the degree of supersaturation) decreases considerably. The only way to clarify this is to perform much longer runs (probably of the order of $10 \mu\text{s}$). At this point this exceeds our computer capacities, but it could be addressed in future work (the computer speed will always increase year after year). The previous reasoning may lead to the conclusion that the direct coexistence simulations may be less reliable than the free energy results. However, this is not completely true. In the direct coexistence simulations, the size of the solution was rather large (i.e., more than 1000 water molecules and more than 100 molecules of salt). When implementing free energy calculations we used a smaller system, containing 270 molecules of water and up to about 40 molecules of NaCl. The reason of this choice of the size is threefold. First, because we wanted to perform the calculations using the same size as was used in our previous study. In this way, we could compare both results and analyze how to perform accurate calculations for a certain system size. In this work, the same technique as in our previous has been used, but the results are more reliable. The second reason is that it is much cheaper to perform very long runs for a small system than for a large one, so that there is also a limit in the computer power even for free energy calculations. Third, Lisal *et al.*³⁵ used exactly the same system size (i.e., 270 water molecules plus a number of NaCl molecules of up to 40) so that this allows a direct comparison with their results. However, neither this work nor the work of Lisal *et al.* have analyzed in detail the possible existence of finite size effects for the chemical potential of NaCl in the solution.³⁵ The size of our system is rather small, so that the hypothesis that there may be finite size effects affecting the value of the chemical potential of NaCl in solution when evaluated from free energy calculations cannot be completely ruled out. It is obvious that further work is needed to clarify these issues. Taking all previous points into account, we have decided to report the final value of the solubility of a certain force field in water as the arithmetic average of the value obtained from free energy calculations and that obtained from direct coexistence simulations, and to assign an error bar to the results which is equal to the distance of the two simulations results to the arithmetic average. This estimated value of the solubility is the central result of this work. From the previous discussion, we found that the JC force field yields a solubility of 5.1(3) m whereas the

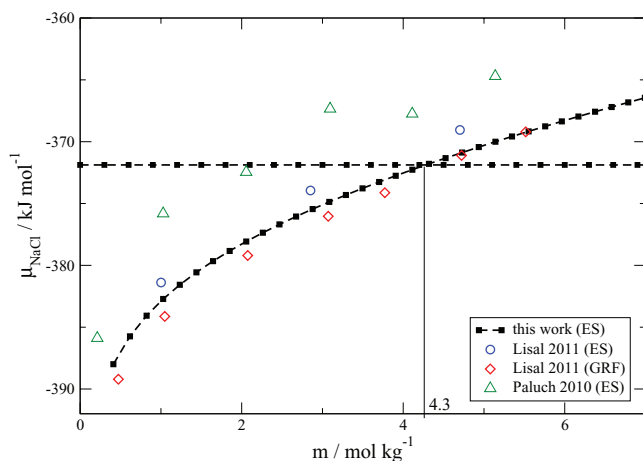


FIG. 7. Chemical potential of NaCl versus molal concentration for the Tosi-Fumi (black dashed line with filled squares) at 298 K and 1 bar. The values computed by Lisal *et al.*³⁵ and Paluch *et al.*³⁴ are also plotted (as indicated in the legend). ES stands for Ewald sums and GRF for generalized reaction field method. The horizontal line represents the solid chemical potential.

solubility of the SD model is of 1.4(5) m. It is clear that the JC model does a good job in predicting the chemical potential of the solid, the chemical potential of the solution, and that of the solubility.

Let us finish the paper by presenting the results for the TF force field. The chemical potential of NaCl for the TF force field obtained in this work are presented in Fig. 7 for the solid and for the NaCl solution. Lisal *et al.* have also computed the chemical potential in the solution for this force field,³⁵ and their values are also presented in Fig. 7. As can be seen, the agreement between the results of this work and those of Lisal *et al.* is quite good. For the solid phase, the chemical potential obtained in this work is practically identical to that reported by us in 2007. The two chemical potential curves intersect at 4.3 m. This value is smaller than our estimate of the solubility reported in 2007, 5.4(8) m (although it is just slightly larger than the error bar of our calculations estimated in 2007). As already discussed, the change between the value of the solubility of this work and that of our 2007 work is due to some methodological improvements that were introduced: longer runs, more values of the coupling parameter λ in the integration of Eq. (13), higher accuracy in the estimate of the densities of the solutions using a fit to describe the densities of the system, and the separation of two contributions when computing the chemical potential. The combined effect of all these changes reduces the solubility by about 1.1 m. The chemical potential of NaCl in the solution obtained in this work agrees quite well with that of Lisal *et al.*³⁵ To estimate solubilities of salts, Lisal *et al.* combine the simulation results for the solution, with the experimental value of the chemical potential of the salt. It is clear from the results of Fig. 7 that would yield an incorrect estimate of the solubility for the TF model, because for this force field the chemical potential of the solid phase is rather different from the experimental value. Notice also that the ions will start to aggregate/precipitate when the chemical potential of the salt in the solution becomes higher than its value in the solid phase (this kind of aggregation has

been studied recently by Alexandre *et al.*)^{65,66} and not when its value becomes higher than the experimental value of the chemical potential of the solid phase. It is of interest to notice that although the TF force field does not reproduce well neither the chemical potential of the solid nor that of the solution, it yields a solubility only slightly worse than the one predicted by the JC force field.

There is still an issue we would like to point out. Paluch *et al.* estimated the solubility of the TF force field to be 0.8 m from free energy calculations.³⁴ The deviation from the value of the solubility reported in this work (4.3 m) is quite large. Let us investigate the origin of the discrepancy. In Fig. 7, the chemical potential of the NaCl solution obtained by Paluch *et al.*³⁴ is compared with the results of this work and those of Lisal *et al.*³⁵ The results of Paluch *et al.*³⁴ are systematically higher than those obtained by Lisal and us. The difference is not large but significant (of about 5 kJ/mol). However, only this difference is not sufficient to explain the difference between the solubility of Paluch (0.8 m) and that of this work (4.3 m). There must be something else. The main difference is that the chemical potential obtained by Paluch *et al.* for the pure NaCl solid is $2 k_B T$ lower than our value. This difference is not due to the accuracy of the free energy calculations of the solid since, as we discussed above, the typical uncertainty in the free energy of the solid phase is of about $0.05 N k_B T$ units. The fact that the difference between the two set of values is $2 k_B T$ is striking. We ascribe the origin of the discrepancy to the inclusion by Paluch *et al.*³⁴ of an additional incorrect $-2 k_B T$ in the ideal gas contribution to the chemical potential of the solid phase. In fact, by differentiating Eq. (11) (with $N_{\text{H}_2\text{O}} = 0$) with respect to N_{NaCl} (at constant T and V), one obtains an expression identical to Eq. (7) of Ref. 34 but for the $-2 k_B T$ term. Notice also that by adding a $-2 k_B T$ to our solid free energies the predicted solubility of the SD and JC would have been extremely small and completely different from the value obtained from direct coexistence simulations.

Let us finish this section with a comparison of the chemical potential of NaCl in water as predicted by the different force fields to the experimental results. This comparison is shown in Fig. 8. As it can be seen, the chemical potential of

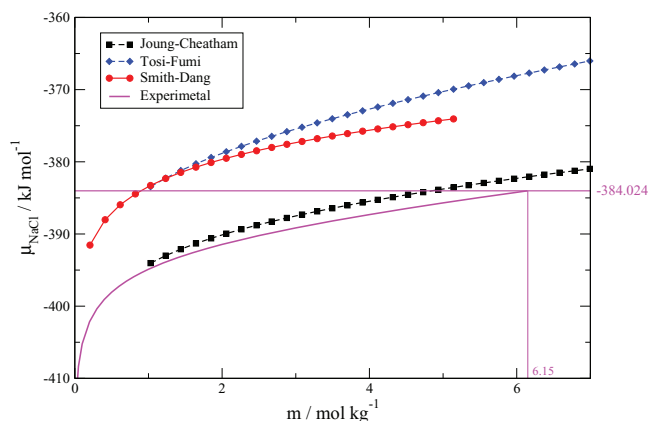


FIG. 8. Chemical potential of NaCl versus molar concentration for all studied models compared to the experimental values. The dashed horizontal line represents the experimental solid chemical potential. Experimental values were obtained with the mean activity coefficients tabulated in Ref. 70 and with the chemical potential at infinite dilution.⁶⁴

the JC force field agrees reasonably well with the experimental results. The results from TF and SD are not so good as they tend to overestimate the chemical potential. The results of the TF and SD are practically identical up to a concentration of 2 m, and are somewhat different for higher concentrations. As it was stated above, the ion–water interaction of the TF and SD force fields are identical. That explains that both models yield practically identical results at low salt concentrations, where the ion–ion interaction play a minor role. It seems that the ion–ion interactions start to affect the magnitude of the chemical potential for concentrations above 2 m. An interesting conclusion of that is that for salts with very low solubility in water (i.e., below 2 m), the ion–ion interactions play a minor role in the chemical potential of the salt in water (although, of course they play a major role in determining the chemical potential of the pure solid phase). That means that for salts with low solubility in water the path to develop a force field is to adjust the ion–ion interactions, first, by forcing the model to reproduce the experimental properties of the solid (density and chemical potential), and afterwards to adjust the ion–water interactions to reproduce the experimental values of the chemical potential of the salt in water at low concentrations (or eventually at infinite dilution). A force field developed in this way will reproduce the chemical potential of both phases and the experimental value of the solubility. When the solubility of the salt in water is high, things are more difficult since the ion–ion interactions will be important not only in determining the chemical potential of the solid phase but also in determining the chemical potential of the salt in water. In any case, all force fields studied here predict a too high chemical potential for the salt in solution as compared to the experimental one. Maybe using other water models that solvate the ions more efficiently, thus reducing the chemical potential, would improve the predictions of the solubility. It seems a sensible approach to adjust the ion–ion interactions using mostly properties of the pure solid and to adjust the ion–water interactions using the properties of the salt in water.^{67–69} It seems that combining rules will not be very useful in the optimization process, and probably the best route is to adjust simultaneously the A–A, X–X, and A–X interactions, rather than to obtain the A–X interactions from combination rules. In this respect, it is interesting to note that in the TF force field the parameters for the A–X interactions were optimized and not obtained from any combination rule. Even assuming that the model to describe water is fixed, and assuming two parameters for each interaction, one needs in total 10 parameters to describe all interactions of the system (A–A, X–X, A–X, A–water, X–water).

CONCLUSIONS

In this work, we have determined the solubility of NaCl in water using computer simulations. Three different force fields were used, and two different methodologies: free energy calculations and direct coexistence simulations. The main conclusions of this work can be summarized as follows:

- The chemical potential of NaCl in the solid phase can be computed with an accuracy of about $0.05 Nk_B T$

units by using the Einstein crystal/molecule methodology. The SD and JC force fields predict nicely the experimental value of the chemical potential of NaCl in the solid phase. The TF force field overestimates the experimental value.

- The JC force field predicts reasonably well the chemical potential of NaCl in water. The predictions from the TF and SD models are quite similar at low concentrations and differ somewhat above 2 m (where ion–ion interactions become more important). The TF and SD force fields overestimate the experimental value of the chemical potential. The chemical potentials for NaCl in water obtained in this work agree quite well with the values recently obtained by Lisal *et al.*³⁵ for the three force fields considered.
- The solubilities of the SD, TF, and JC models evaluated from free energy calculations are 0.9 m, 4.3 m, and 4.8 m, respectively. The experimental value is 6.15 m. The solubility changes quite significantly with the force field. The SD predicts well the chemical potential of the solid and poorly that of the solution, the final result is a poor estimate of the solubility. The JC predicts quite well the chemical potential of the solid and reasonably well the chemical potential of the solution, so that it yields a reasonable estimate of the solubility. The TF does not predict correctly neither the chemical potential of the solid nor that of the fluid phase but still is able to yield a reasonable prediction for the solubility.
- The solubilities of the SD and JC have also been determined from direct coexistence simulations. Runs of $2.8 \mu s$ were needed to reach a plateau in the concentration of salt. The solubilities found from this route were respectively, 1 m and 0.7 m above the values from free energy calculations. Taking into account the difficulties encountered in all the calculations, we find the agreement with the free energy route reasonable. However, further work is needed to clarify the origin of the difference (longer runs may be needed in the direct coexistence simulations, or finite size effects in the free energy calculations can affect the value of the chemical potential of the salt in solution). For the time being we recommended value of the solubility is 5.1(3) m for the JC force field and 1.4(5) m for the SD force field.
- The solubility of the JC and SD models can be estimated quite well by computing the chemical potential of the solution and assuming that the chemical potential of the model in the solid phase is identical to the experimental value. That was the approach followed by Lisal *et al.*³⁵ which seems to yield correct results for these two force fields. However, this approach would yield an incorrect value of the solubility for the TF force field, as the chemical potential for the TF force field in the solid phase does not correspond to the experimental value. The assumption that the chemical potential of the solid phase matches the experimental value (implicitly adopted by Lisal *et al.*)³⁵ will only work for certain force fields, but it will fail for others.

- The solubility for the TF force field obtained in this work (4.3 m), somewhat lower than that obtained in our previous work (5.4(8) m). Longer runs and a more sensible data analysis have increased the accuracy of the calculations. The solubility found in this work still deviates significantly from the estimate reported by Paluch *et al.*³⁴ (0.8 m). This is due to a higher value of the chemical potential of NaCl in water reported by Paluch *et al.* as compared to the value reported by Lisal *et al.*³⁵ and that reported in this work. Second and more significantly, the chemical potential of the solid phase reported by Paluch is $2 k_B T$ units lower than the value reported here.

The reader may have the impression that finally there is a reliable force field for NaCl the Joung–Cheatham model. From the results presented so far this is a reasonable conclusion. However, things are not that simple. By using direct coexistence simulations we have determined the melting point of NaCl (i.e., the equilibrium between pure NaCl in the solid phase and pure NaCl in the liquid phase). We have found⁵³ that the melting point was 1286(10) K which is above the experimental value of 1074 K. Thus, even though the JC force field describes well the experimental value of the chemical potential of the NaCl solid at room temperature, it yields an incorrect melting point (either because the performance of the model deteriorates at high temperatures or because the model fails to describe the NaCl melt). Remember that the TF force reproduces almost exactly the melting point of NaCl.^{51,71} Definitely, things are complicated and it is difficult to find a force field that matches all these properties. Hopefully one should expect progress on this area of research in the future.

The studies of the solubility of salts in water are scarce, and basically there are only 7 papers dealing with this issue, the seminal work of Ferrario *et al.*,³² the two papers of Lisal *et al.*,^{35,72} the paper of Paluch *et al.*,³⁴ the work of Joung and Cheatham,⁴⁴ and the two studies of our group, this paper and our previous work.³³ It is clear that the interest in the problem has increased significantly in the last five years. Likely more studies will soon come on this interesting problem. It would be of interest to develop a force field for NaCl in water able to describe the experimental value of the solubility, and also develop models for ions obtained either from first principles⁷³ or from polarizable models.⁷⁴

Note added in proof: After this paper was finished a paper by Moucka *et al.* has been published.⁷⁵ The chemical potential of the NaCl (both in the solid phase and into water solution) for the TF and JC force fields of Ref. 75 are in agreement with those presented in this work.

ACKNOWLEDGMENTS

This work was funded by Grant Nos. FIS2010-16159, from the DGI (Spain), MODELICO-P2009/ESP/1691 from the CAM, and 910570 from the UCM. J. L. Aragones would like to thank the MEC by the award of FPI pre-doctoral grant. We would like to thank C. McBride for a critical reading of the paper and J. L. F. Abascal for helpful discussions.

APPENDIX A: EVALUATING THE CONTRIBUTION OF THE G_1 TERM TO THE CHEMICAL POTENTIAL

The chemical potential of NaCl in the solution is given by the expression

$$\mu_{\text{NaCl}}^{\text{solution}} = \left(\frac{\partial G_{\text{solution}}}{\partial N_{\text{NaCl}}} \right)_{T,p,N_{\text{H}_2\text{O}}}, \quad (\text{A1})$$

where G_{solution} is the Gibbs free energy (see Eq. (14)). We have split G_{solution} in two terms, the first one $G_1 = A_{\text{solution}}^{\text{id}}$ contains the ideal gas contribution to the Helmholtz free energy of the system. The second one G_2 contained the other contributions to the Gibbs free energy, the residual contribution to the Helmholtz free energy and the pV_{solution} term. The contribution of the G_1 term to the chemical potential will be denoted as $\mu_{\text{NaCl},1}^{\text{solution}}$ and is given by

$$\mu_{\text{NaCl},1}^{\text{solution}} = \left(\frac{\partial A_{\text{solution}}^{\text{id}}}{\partial N_{\text{NaCl}}} \right)_{T,p,N_{\text{H}_2\text{O}}}. \quad (\text{A2})$$

The term $A_{\text{solution}}^{\text{id}}$ is given by Eq. (11). By taking the derivative of $A_{\text{solution}}^{\text{id}}$ with respect to the number of molecules of NaCl N_{NaCl} while keeping T and p constant, one obtains

$$\left(\frac{\partial (A_{\text{solution}}^{\text{id}}/k_B T)}{\partial N_{\text{NaCl}}} \right)_{T,p,N_{\text{H}_2\text{O}}} = 2 \ln(\rho_{\text{NaCl}}) - 2 + V \times (2\rho'_{\text{NaCl}} + \rho'_{\text{H}_2\text{O}}), \quad (\text{A3})$$

where $\rho'_{\text{H}_2\text{O}}$ stands for $\left(\frac{\partial \rho_{\text{H}_2\text{O}}}{\partial N_{\text{NaCl}}} \right)_{T,p,N_{\text{H}_2\text{O}}}$, being $\rho_i = \frac{N_i}{V}$ the number density of component i . The term $\rho'_{\text{H}_2\text{O}}$ can be written as

$$\begin{aligned} \left(\frac{\partial \rho_{\text{H}_2\text{O}}}{\partial N_{\text{NaCl}}} \right)_{T,p,N_{\text{H}_2\text{O}}} &= \frac{\partial \left(\frac{N_{\text{H}_2\text{O}}}{V} \right)}{\partial N_{\text{NaCl}}} = - \frac{N_{\text{H}_2\text{O}} \left(\frac{\partial V}{\partial N_{\text{NaCl}}} \right)}{V^2} \\ &= - \frac{N_{\text{H}_2\text{O}} \bar{V}}{V^2}, \end{aligned} \quad (\text{A4})$$

where V stands for the volume of the system and \bar{V} stands for the partial molar volume of NaCl. Similarly, the term ρ'_{NaCl} , that corresponds to $\left(\frac{\partial \rho_{\text{NaCl}}}{\partial N_{\text{NaCl}}} \right)$ can be written as

$$\left(\frac{\partial \rho_{\text{NaCl}}}{\partial N_{\text{NaCl}}} \right)_{T,p,N_{\text{H}_2\text{O}}} = \frac{1}{V} - \frac{N_{\text{NaCl}} \bar{V}}{V^2}. \quad (\text{A5})$$

Taking into account the expressions for ρ'_{NaCl} and $\rho'_{\text{H}_2\text{O}}$, the last term of Eq. (A3) can be written as

$$(2\rho'_{\text{NaCl}} + \rho'_{\text{H}_2\text{O}}) = \frac{1}{V} \left(\frac{-2N_{\text{NaCl}} \bar{V}}{V} - \frac{N_{\text{H}_2\text{O}} \bar{V}}{V} + 2 \right) \quad (\text{A6})$$

so that the final expression for $\mu_{\text{NaCl},1}^{\text{solution}}$ is

$$\left(\frac{\partial (A_{\text{solution}}^{\text{id}}/k_B T)}{\partial N_{\text{NaCl}}} \right)_{T,p,N_{\text{H}_2\text{O}}} = 2 \ln(\rho_{\text{NaCl}}) - \bar{V} (2\rho_{\text{NaCl}} + \rho_{\text{H}_2\text{O}}). \quad (\text{A7})$$

APPENDIX B: CONVERTING THE CHEMICAL POTENTIAL TO EXPERIMENTAL UNITS

Let us describe briefly how to convert chemical potentials from the units of this work (which implicitly used 1 \AA for the thermal de Broglie wavelength and one for the internal partition function to one for all species) to the units used in experimental work which are also the units used by Lisal *et al.*³⁵ when describing NaCl models in water. First, one should use the experimental values of the standard chemical potentials of Na^+ and Cl^- , as taken from NIST-JANAF (Ref. 64) tables which amount to ($\mu_{\text{Na}^+} = 574.317 \text{ kJ mol}^{-1}$ and $\mu_{\text{Cl}^-} = -240.167 \text{ kJ mol}^{-1}$). Implicitly our choice of setting the intramolecular partition function for all species equal to one means that these values were zero in our criterion. We can simply add the sum of these two terms to our chemical potentials. The second point is that our reference state is a system with a particle per \AA^3 , whereas experimentally the reference state is the volume occupied by a molecule per (kT/p^0) where $p^0 = 1 \text{ bar}$ is the reference pressure. Therefore, the chemical potential of this work can be converted into experimental units by simply adding the constant C

$$C(\text{kJ/mol}) = \mu_{\text{Na}^+}(\text{kJ/mol}) + \mu_{\text{Cl}^-}(\text{kJ/mol}) + \frac{2RT}{1000} \ln(k_B T 10^{25}), \quad (\text{B1})$$

where the 10^{25} term arises from a 10^{30} term to convert from m^3 to \AA^3 divided by a 10^5 term which 1 bar of pressure in Pascals. By replacing the value of R (8.314 J/mol/K) and k_B ($1.3805 \cdot 10^{-23} \text{ J/K}$), one obtains $C = 386.8 \text{ kJ/mol}$. Thus, the chemical potentials of this work can be converted into the units used in experimental work by simply adding this constant C.

APPENDIX C: COMPARING OUR MONTE CARLO TO MOLECULAR DYNAMICS

We have also compared the results obtained using our own Monte Carlo program to those obtained from molecular dynamic simulations obtained running GROMACS. In both cases, we used NpT simulations at 298 K and 1 bar for a solution composed by 270 water molecules and 10 NaCl molecules (20 ions), $N = 290$. Results are shown in Table XI for SD and JC force fields (for a solution of NaCl

TABLE XI. Comparison between number densities and residual internal energies (per mol of particles) obtained with GROMACS and with our MC program for the JC force field at 298 K and 1 bar.

Method	U (kcal/mol)	ρ (N/\AA^{-3})
Joung–Cheatham		
GROMACS	-17.01	0.0347
MC	-17.02	0.0348
Smith–Dang		
GROMACS	-16.86	0.0344
MC	-16.88	0.0345

in water). As it can be the agreement for the densities and internal energies is quite good.

APPENDIX D: CHEMICAL POTENTIAL OF A BINARY MIXTURE USING A SIMPLE MODEL

To show the correctness of the thermodynamic route used in this work to determine the chemical potential of NaCl in water, it is useful to consider a very simple model, for which the calculations can be implemented easily. We shall consider a binary mixture of hard bodies described with a virial expansion, truncated at the second virial coefficient. The expression for the compressibility factor ($Z = p/(\rho kT)$) of the mixture is given by

$$Z = 1 + B_2 \rho, \quad (\text{D1})$$

where $\rho = (N/V) = (N_1 + N_2)/V$ is the total number density of components 1 and 2 and the second virial coefficient of the mixture is defined as

$$B_2 = \sum_i \sum_j B_{ij} x_i x_j, \quad (\text{D2})$$

x_i being the molar fraction of component i and B_{ij} the second virial coefficient between a molecule of type i and a molecule of type j . Since we are assuming hard bodies the virial coefficients will always be positive. The residual contribution to the Helmholtz free energy can be obtained from the expression

$$A^{res}/(NkT) = \int_0^\rho \frac{(Z-1)}{\rho'} d\rho' = B_2 \rho. \quad (\text{D3})$$

The ideal term to the Helmholtz free energy of the mixture is given by

$$A^{id}/(NkT) = x_1 \ln(\rho_1 \sigma^3) + x_2 \ln(\rho_2 \sigma^3) - 1, \quad (\text{D4})$$

where we have assumed that the de Broglie thermal length of the two species is identical and we have set its value to a certain characteristic molecular length σ that will be used as unit of length $\sigma = 1$.

By adding together the ideal and residual terms one obtains for A

$$A = N_1 kT \ln(\rho_1 \sigma^3) + N_2 kT \ln(\rho_2 \sigma^3) - N_1 kT - N_2 kT + NkT B_2 \rho. \quad (\text{D5})$$

Let us compute the chemical potential of component 2 from the expression

$$\mu_2 = \left(\frac{\partial A}{\partial N_2} \right)_{T, V, N_1}. \quad (\text{D6})$$

Evaluating the derivatives analytically, one obtains

$$\mu_2 = kT \ln(\rho_2 \sigma^3) + 2kT(B_{11} \rho_2 + B_{12} \rho_1). \quad (\text{D7})$$

The chemical potential can also be obtained from the derivative of the Gibbs free energy $G = A^{id} + A^{res} + pV$ with respect to N_2 at constant T and p

$$\mu_2 = \left(\frac{\partial G}{\partial N_2} \right)_{T, p, N_1}, \quad (\text{D8})$$

where the derivative is performed at constant pressure. For this simple mixture, the volume of the system at a certain T, p ,

N_1 , and N_2 can be obtained by simply solving a second order polynomial equation. Once this is done, the A^{id} , A^{res} , and pV terms are computed trivially from the expression described above. That allows one to compute the Gibbs free energy of the system G as a function of N_2 (for a certain fixed values of T , p , N_1). The derivative of G with respect to N_2 provides the chemical potential μ_2 from this route. Obviously, the two routes (differentiating A with respect to N_2 while keeping T , V , and N_1 constant and differentiating G with respect to N_2 while keeping T , p , and N_1 constant should be equivalent and should yield the same value of the chemical potential). Let us consider a system with $B_{11}/\sigma^3 = 1$, $B_{22}/\sigma^3 = 3$, $B_{12}/\sigma^3 = 1.6$. Let us assume that $N_1 = 270$ and $N_2 = 50$ and $p/(kT/\sigma^3) = 1$. From the derivative of A , at constant T , V , and N_1 we obtained $\mu_2/(kT) = -0.26024$ (-2.39108 being the contribution of the ideal gas term and 2.13084 of the residual free energy term). From the derivative of G , at constant T , p , and N_1 we obtained $\mu_2/(kT) = -0.26024$ (-3.68794 from the ideal gas term, 1.21385 from the residual free energy term, and 2.21385 from the pV term). Obviously the chemical potential is the same regardless of the thermodynamic route. Notice that the derivative of A is done at constant T , V , and N_1 , and the derivative of G is done at constant T , p , and N_1 . In this work, we have always evaluated the chemical potential by performing derivatives at constant T , p , and N_1 (i.e., the number of molecules of water).

- ¹D. Williams, *Chem. Rev.* **72**, 203 (1972).
- ²G. S. Manning, *Q. Rev. Biophys.* **11**, 179 (1978).
- ³D. Klein, P. Moore, and T. Steitz, *RNA* **10**, 1366 (2004).
- ⁴J. Viereg, W. Cheng, C. Bustamante, and I. Tinoco, *J. Am. Chem. Soc.* **129**, 14966 (2007).
- ⁵F. Sinibaldi, B. D. Howes, G. Smulevich, C. Ciaccio, M. Coletta, and R. Santucci, *JBIC, J. Biol. Inorg. Chem.* **8**, 663 (2003).
- ⁶M. A. Carignano, E. Baskaran, P. B. Shepson, and I. Szleifer, *Ann. Glaciol.* **44**, 44A195 (2006).
- ⁷D. Zahn, *Phys. Rev. Lett.* **92**, 040801 (2004).
- ⁸I. Okada, Y. Namiki, H. Uchida, M. Aizawa, and K. Itatani, *J. Mol. Liq.* **118**, 131 (2005).
- ⁹H. Shinto, T. Sakakibara, and K. Higashitani, *J. Phys. Chem. B* **102**, 1974 (1998).
- ¹⁰Y. Yang, S. Meng, L. F. Xu, and E. G. Wang, *Phys. Rev. E* **72**, 012602 (2005).
- ¹¹B. Wolf and S. Hanlon, *Biochemistry* **14**, 1661 (1975).
- ¹²C. C. Hardin, E. Henderson, T. Watson, and J. K. Prosser, *Biochemistry* **30**(18), 4460 (1991).
- ¹³D. Corradini, M. Rovere, and P. Gallo, *J. Chem. Phys.* **132**, 134508 (2010).
- ¹⁴D. Corradini, P. Gallo, and M. Rovere, *J. Phys. Condens. Matter* **22**, 284104 (2010).
- ¹⁵D. Corradini, P. Gallo, and M. Rovere, *J. Chem. Phys.* **130**, 154511 (2009).
- ¹⁶D. Corradini, M. Rovere, and P. Gallo, *J. Phys. Chem. B* **115**, 1461 (2011).
- ¹⁷D. Argyris, D. R. Cole, and A. Striolo, *ACS Nano* **4**, 2035 (2010).
- ¹⁸Y. S. Lin, B. M. Auer, and J. L. Skinner, *J. Chem. Phys.* **131**, 144511 (2009).
- ¹⁹M. Salanne, C. Simon, P. Turq, and P. A. Madden, *J. Phys. Chem. B* **112**, 1177 (2008).
- ²⁰Y. Laudernet, T. Cartiailler, P. Turq, and M. Ferrario, *J. Phys. Chem. B* **107**, 2354 (2003).
- ²¹M. A. Carignano, P. B. Shepson, and I. Szleifer, *Chem. Phys. Lett.* **436**, 99 (2007).
- ²²L. Vrbka and P. Jungwirth, *Phys. Rev. Lett.* **95**, 148501 (2005).
- ²³L. Vrbka and P. Jungwirth, *J. Mol. Liq.* **134**, 64 (2007).
- ²⁴S. Bauerecker, P. Ulbig, V. Buch, L. Vrbka, and P. Jungwirth, *J. Phys. Chem. C* **112**, 7631 (2008).
- ²⁵J. Vincze, M. Valisko, and D. Boda, *J. Chem. Phys.* **133**, 154507 (2010).
- ²⁶A. P. Hynninen and A. Z. Panagiotopoulos, *Mol. Phys.* **106**, 2039 (2008).
- ²⁷T. Straatsma and H. Berendsen, *J. Chem. Phys.* **89**, 5876 (1988).
- ²⁸A. Lyubartsev, O. Forrisdahl, and A. Laaksonen, *J. Chem. Phys.* **108**, 227 (1998).
- ²⁹R. Lynden-Bell, J. Rasaiah, and J. Noworyta, *Pure Appl. Chem.* **73**, 1721 (2001).
- ³⁰G. Hummer, L. R. Pratt, and A. E. Garcia, *J. Phys. Chem.* **100**, 1206 (1996).
- ³¹E. Smith, T. Bryk, and A. Haymet, *J. Chem. Phys.* **123**, 034706 (2005).
- ³²M. Ferrario, G. Ciccotti, E. Spohr, T. Cartiailler, and P. Turq, *J. Chem. Phys.* **117**, 4947 (2002).
- ³³E. Sanz and C. Vega, *J. Chem. Phys.* **126**, 014507 (2007).
- ³⁴A. S. Paluch, S. Jayaraman, J. K. Shah, and E. J. Maginn, *J. Chem. Phys.* **133**, 124504 (2010).
- ³⁵F. Moucka, M. Lissal, J. Skvor, J. Jirsak, I. Nezbeda, and W. Smith, *J. Phys. Chem. B* **115**, 7849 (2011).
- ³⁶D. Frenkel and A. J. C. Ladd, *J. Chem. Phys.* **81**, 3188 (1984).
- ³⁷C. Vega and E. G. Noya, *J. Chem. Phys.* **127**, 154113 (2007).
- ³⁸E. G. Noya, M. M. Conde, and C. Vega, *J. Chem. Phys.* **129**, 104704 (2008).
- ³⁹A. J. C. Ladd and L. Woodcock, *Chem. Phys. Lett.* **51**, 155 (1977).
- ⁴⁰A. J. C. Ladd and L. Woodcock, *Mol. Phys.* **36**, 611 (1978).
- ⁴¹O. A. Karim and A. D. J. Haymet, *J. Chem. Phys.* **89**, 6889 (1988).
- ⁴²R. G. Fernandez, J. L. F. Abascal, and C. Vega, *J. Chem. Phys.* **124**, 144506 (2006).
- ⁴³C. Vega, M. Martin-Conde, and A. Patrykiewicz, *Mol. Phys.* **104**, 3583 (2006).
- ⁴⁴I. Joung and T. Cheatham, *J. Phys. Chem. B* **113**, 13279 (2009).
- ⁴⁵I. Joung and T. Cheatham, *J. Phys. Chem. B* **112**, 9020 (2008).
- ⁴⁶H. J. C. Berendsen, J. R. Grigera, and T. P. Straatsma, *J. Phys. Chem.* **91**, 6269 (1987).
- ⁴⁷J. E. Mayer, *J. Chem. Phys.* **1**, 270 (1933).
- ⁴⁸M. L. Huggins and J. E. Mayer, *J. Chem. Phys.* **1**, 643 (1933).
- ⁴⁹F. Fumi and M. Tosi, *J. Phys. Chem. Solids* **25**, 31 (1964).
- ⁵⁰D. Adams and I. McDonald, *J. Phys. C* **25**, 00045 (1964).
- ⁵¹J. Anwar, D. Frenkel, and M. G. Noro, *J. Chem. Phys.* **118**, 728 (2003).
- ⁵²C. Valeriani, E. Sanz, and D. Frenkel, *J. Chem. Phys.* **122**, 194501 (2005).
- ⁵³J. L. Aragonés, C. Valeriani, E. Sanz, and C. Vega, "Calculation of the melting point of alkali halides by means of computer simulations," *J. Chem. Phys.* (submitted).
- ⁵⁴D. E. Smith and L. X. Dang, *J. Chem. Phys.* **100**, 3757 (1994).
- ⁵⁵L. Dang and D. E. Smith, *J. Chem. Phys.* **99**, 6950 (1993).
- ⁵⁶C. Vega, E. Sanz, E. G. Noya, and J. L. F. Abascal, *J. Phys. Condens. Matter* **20**, 153101 (2008).
- ⁵⁷L. L. Lee, *Molecular Thermodynamics of Nonideal Fluids* (Butterworths, 1988).
- ⁵⁸J. Kolafa and I. Nezbeda, *Fluid Phase Equilib.* **100**, 1 (1994).
- ⁵⁹D. V. der Spoel, E. Lindahl, B. Hess, G. Groenhof, A. E. Mark, and H. J. C. Berendsen, *J. Comput. Chem.* **26**, 1701 (2005).
- ⁶⁰G. Bussi, D. Donadio, and M. Parrinello, *J. Chem. Phys.* **126**, 014101 (2007).
- ⁶¹M. Parrinello and A. Rahman, *J. Appl. Phys.* **52**, 7182 (1981).
- ⁶²U. Essmann, L. Perera, M. L. Berkowitz, T. Darden, H. Lee, and L. G. Pedersen, *J. Chem. Phys.* **103**, 8577 (1995).
- ⁶³B. Hess, H. Bekker, H. J. C. Berendsen, and J. G. E. M. Fraaije, *J. Comput. Chem.* **18**, 1463 (1997).
- ⁶⁴M. W. Chase, *NIST-JANAF Thermochemical Tables*, Journal of Physical and Chemical Reference Data Monograph Vol. 9 (American Institute of Physics, Woodbury, 1998).
- ⁶⁵J. Alejandre and J. P. Hansen, *Phys. Rev. E* **76**, 061505 (2007).
- ⁶⁶J. Alejandre, G. A. Chapela, F. Bresme, and J. P. Hansen, *J. Chem. Phys.* **130**, 174505 (2009).
- ⁶⁷M. M. Reif and P. H. Huenenberger, *J. Chem. Phys.* **134**, 144104 (2011).
- ⁶⁸I. Gladich, P. Shepson, I. Szleifer, and M. Carignano, *Chem. Phys. Lett.* **489**, 113 (2010).
- ⁶⁹M. Fyta and R. R. Netz, *J. Chem. Phys.* **136**, 124103 (2012).
- ⁷⁰D. Wagman, *J. Phys. Chem. Ref. Data* **11**(2), 1996 (1982).
- ⁷¹J. Anwar and D. Zahn, *Angew. Chem., Int. Ed.* **50**, 1996 (2011).
- ⁷²M. Lissal, W. Smith, and J. Kolafa, *J. Phys. Chem. B* **109**, 12956 (2005).
- ⁷³M. Cavallari, C. Cavazzoni, and M. Ferrario, *Mol. Phys.* **102**, 959 (2004).
- ⁷⁴E. Wernersson and P. Jungwirth, *J. Chem. Theory Comput.* **6**, 3233 (2010).
- ⁷⁵F. Moucka, M. Lissal, and W. R. Smith, *J. Phys. Chem. B* **116**, 5468 (2012).